

VLE and VLLE Measurements of Dimethyl Ether Containing Systems

Torben Laursen, Peter Rasmussen, and Simon Ivar Andersen*

Engineering Research Centre IVC-SEP, Department of Chemical Engineering,
The Technical University of Denmark, DK-2800 Lyngby, Denmark

The present work describes a method that allows rapid measurement of both VLE and VLLE isotherms. Samples of the various phases are taken from a high-pressure autoclave equipped with windows using a movable needle. The samples are sent directly into a GC that is calibrated using pure compounds. The procedure allows for the measurement of a full isotherm with 5 to 10 data points for all phases during one working week. The method has been validated by measuring the systems $\text{CO}_2 + \text{CH}_3\text{OH}$ and $\text{CO}_2 + (\text{CH}_3)_2\text{O}$ and comparing with literature data. Thereafter, a range of systems composed of the five components N_2 , CO_2 , $(\text{CH}_3)_2\text{O}$, H_2O , and CH_3OH has been measured. This work contains new experimental data for the systems $\text{CO}_2 + \text{CH}_3\text{OH}$, $\text{N}_2 + (\text{CH}_3)_2\text{O}$, $\text{CO}_2 + (\text{CH}_3)_2\text{O}$, $\text{N}_2 + (\text{CH}_3)_2\text{O} + \text{H}_2\text{O}$, $\text{CO}_2 + (\text{CH}_3)_2\text{O} + \text{H}_2\text{O}$, $\text{CO}_2 + (\text{CH}_3)_2\text{O} + \text{H}_2\text{O} + \text{CH}_3\text{OH}$, $\text{N}_2 + (\text{CH}_3)_2\text{O} + \text{H}_2\text{O} + \text{CH}_3\text{OH}$, and $\text{N}_2 + \text{CO}_2 + (\text{CH}_3)_2\text{O} + \text{H}_2\text{O} + \text{CH}_3\text{OH}$, in the temperature range 25 to 45 °C and the pressure range 3 to 105 bar.

Introduction

Dimethyl ether ($(\text{CH}_3)_2\text{O}$) (DME) may have a future as a replacement for engine fuel obtained from fossil reserves.¹ To produce DME on a large scale, a full knowledge of the many phase equilibria involved is required. Previously, a number of VLE data have been published,^{2–6} but the only VLLE data found are for the system $(\text{CH}_3)_2\text{O} + \text{H}_2\text{O}$ limited to 10 bar.⁵ This work focuses on the phase behavior found in systems made by combinations of the five components N_2 , CO_2 , $(\text{CH}_3)_2\text{O}$, H_2O , and CH_3OH , since all five components are involved when producing DME. Some of these systems show both VLE and VLLE behavior while others show only VLE in the experimental pressure and temperature ranges. The equipment used allows for measurement of the composition of all the phases present in the cell, and new data are presented for eight different combinations of the five components.

Experimental Section

The experimental apparatus is based on a high-pressure autoclave equipped with two windows, a movable sample needle, and valves for performing on-line sampling from the cell. The equipment can be used to measure both VLE and VLLE, but not LLE, for safety reasons.

A schematical outline of the equipment can be found in Figure 1.

Equilibrium Cell. The vapor–liquid equilibrium measurements are done in a Top autoclave model number 1030.0000 with a volume of 570 mL. It is equipped with two sapphire windows for observation of the cell content. Stirring is carried out mechanically. The stirrer is mounted through the lid of the cell and is driven using a magnetic coupling (Maxon DC motor model P10). The temperature is measured using a Eurotherm 2416 PT100 with a resolution of ± 0.1 K placed in a well in the cell, and through the lid. Pressure is measured by using a

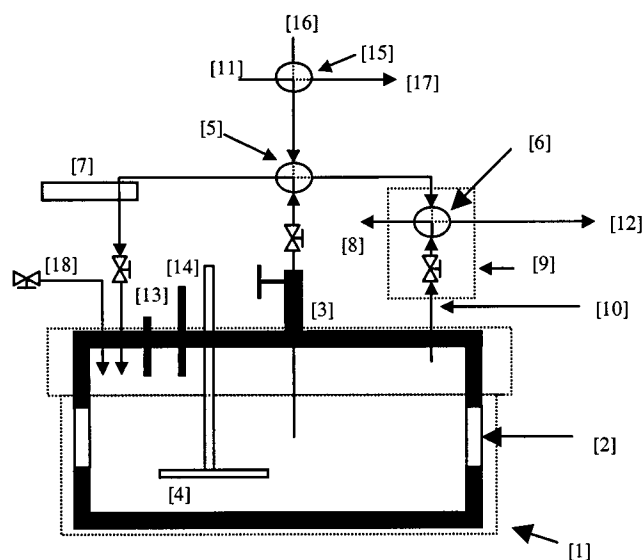


Figure 1. Schematic diagram of the VLLE experimental apparatus: 1, autoclave; 2, window; 3, movable liquid sample needle; 4, mechanical stirrer; 5, liquid sampling valve; 6, vapor sampling valve; 7, liquid pump; 8, waste; 9, heated box; 10, heated pipe; 11, He inlet; 12, line to GC; 13, temperature sensor; 14, pressure gauge; 15, calibration sampling valve; 16, inlet to calibration valve; 17, waste from calibration loop; 18, inlet to cell.

MEX3D20B35 from Bourdon with a resolution of ± 0.1 bar. Thermostating is obtained using four heating rods mounted into the side of the autoclave and additional heating on the top of the lid of the autoclave.

Sample Needle. The autoclave is equipped with a movable sample needle from Top Industries, so that samples can be taken from any liquid phase present in the cell. The sample needle is constructed similarly to a manual bicycle pump, taking advantage of a difference in piston area in order to operate over a large pressure difference. The needle is held in place using compressed air, and by

* Corresponding author. E-mail: sia@kt.dtu.dk.

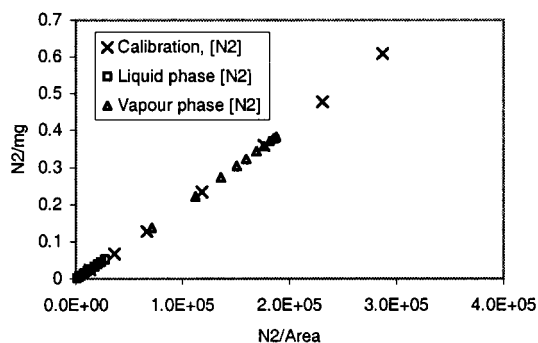


Figure 2. Example of a calibration curve for N_2 , including the distribution of the points for the system N_2 (1) + $(CH_3)_2O$ (2) at $45.0\text{ }^\circ\text{C}$.

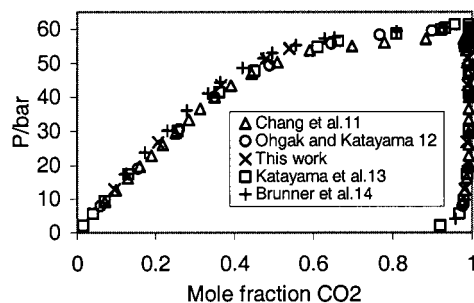


Figure 3. Comparison between literature data for the system CO_2 (1) + CH_3OH (2) at $25.0\text{ }^\circ\text{C}$ and data obtained in this work.

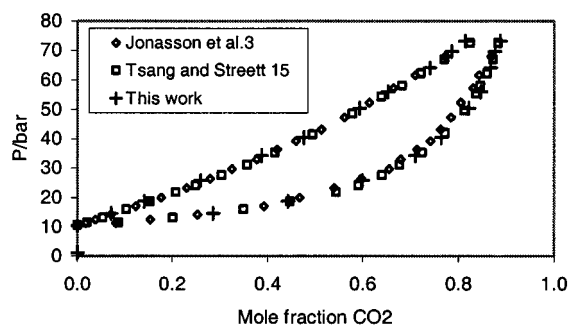


Figure 4. Comparison between literature data and data obtained in this work for the system CO_2 (1) + $(CH_3)_2O$ (2) at $47.0\text{ }^\circ\text{C}$.

Table 1. Materials Used, Supplier, and Purity

material	supplier	purity/%
carbon dioxide	Hede Nielsen	99.995
nitrogen	Hede Nielsen	99.995
dimethyl ether	Sigma Aldrich	99.7
water	J.T. Baker	99.998
methanol	J.T. Baker	99.8

adjusting the pressure of the compressed air to a level that just matches the pressure in the cell given the area difference, the needle can be moved using little force and without any leaks.

Pump. The circulation of the liquid is achieved using a pump of type LEWA FC M400.

Sampling Valves. The system is equipped with three Rheodyne sample valves, all placed in series with a He stream that enters the GC. The liquid valve (model 7410) is equipped with a $0.5\ \mu\text{L}$ loop, and the vapor valve (model 7010) is mounted with a $500\ \mu\text{L}$ loop. The calibration valve (model 7410) is not mounted with a loop of fixed size. The maximum operating temperature and pressure of the liquid and vapor valves are $125\text{ }^\circ\text{C}$, 340 bar and $150\text{ }^\circ\text{C}$, 340 bar, respectively.

Table 2. Compositions of the Liquid (x_1) and Vapor (y_1) Phases at the Pressure P for the System CO_2 (1) + CH_3OH (2)

x_1	y_1	P/bar	x_1	y_1	P/bar
$T = 25.0\text{ }^\circ\text{C}$					
0.0946	0.9824	13.0	0.4799	0.9901	51.3
0.2061	0.9873	26.8	0.5399	0.9897	54.4
0.3667	0.9902	43.5	0.5379	0.9895	54.2
$T = 30.0\text{ }^\circ\text{C}$					
0.0748	0.9756	12.4	0.4662	0.9888	54.8
0.2032	0.9871	30.8	0.4586	0.9893	55.0
0.1951	0.9875	30.7	0.4552	0.9896	55.1
0.3248	0.9896	44.8			
$T = 40.0\text{ }^\circ\text{C}$					
0.0887	0.9799	15.9	0.3448	0.9894	53.8
0.1693	0.9871	28.8	0.4251	0.9883	63.4
0.2486	0.9889	41.4			

Table 3. Compositions of the Liquid (x_1) and Vapor (y_1) Phases at the Pressure P for the System CO_2 (1) + $(CH_3)_2O$ (2)

x_1	y_1	P/bar	x_1	y_1	P/bar
$T = 25.0\text{ }^\circ\text{C}$					
0.0000	0.0000	6.0	0.6164	0.8875	34.6
0.2597	0.6857	16.6	0.7261	0.9190	41.2
0.4546	0.8179	25.6	0.8478	0.9542	49.8
$T = 35.5\text{ }^\circ\text{C}$					
0.0000	0.0000	7.9	0.4289	0.7874	31.1
0.1023	0.4052	13.0	0.5491	0.8476	38.8
0.1954	0.5821	17.7	0.6515	0.8791	45.8
0.2272	0.5908	19.3	0.7154	0.8986	50.8
0.3443	0.7292	25.7	0.7939	0.9221	57.3
$T = 47.0\text{ }^\circ\text{C}$					
0.0000	0.0000	10.3	0.5932	0.8218	50.3
0.0708	0.2862	14.5	0.6536	0.8476	55.9
0.1412	0.4432	18.7	0.8140	0.8886	73.2
0.2590	0.5992	25.6	0.7869	0.8769	69.7
0.3880	0.7106	34.3	0.7414	0.8684	64.1
0.4768	0.7651	40.4			

Gas Chromatograph (GC). The samples taken were analyzed using a Carlo Erba HRGC 5300 GC equipped with a TCD detector (HWD 430). The columns used were 3 m 1/8 in. stainless steel with a 2.1 mm i.d. filled with HayeSep T mesh 80/100. The oven and injection zone temperature was set to $140\text{ }^\circ\text{C}$, and the He flow was set to $19\text{ mL}\cdot\text{min}^{-1}$ for the analysis column and $19\text{ mL}\cdot\text{min}^{-1}$ for the reference column. Both flows are set at an oven temperature of $70\text{ }^\circ\text{C}$. The TCD was set to $200\text{ }^\circ\text{C}$, and the filaments were set to $220\text{ }^\circ\text{C}$.

GC Calibration. Calibration of the GC was performed by injecting different amounts of the pure component and making a regression of the amount versus the area; see Figure 2. When the compound is a liquid at room conditions, a manual SEG $1.0\ \mu\text{L}$ syringe was used to inject samples in the range 0.1 to $1.0\ \mu\text{L}$ in order to make the calibration curve. The numbers used are an average of two injections. It was found that if the syringe used was equipped with a plunger support, the standard deviation of the injection would be on average 0.5% and about 5% without, so all liquid calibrations were done using a plunger support.

If the compound is a gas, loops in the size range 10 to $500\ \mu\text{L}$ were used. The loops were mounted onto the calibration valve. The sample was taken from a gas cylinder and flowed through the loops and into a water beaker. The loops used were calibrated using pure water combined with gravimetry. The uncertainty of the size of the loop was found to be within $0.5\ \mu\text{L}$. The numbers used were an average of two injections, and the standard deviation was on average 0.1%.

Table 4. Compositions of the Liquid (x_1) and Vapor (y_1) Phases at the Pressure P for the System N_2 (1) + $(CH_3)_2O$ (2)

x_1	y_1	P/bar	x_1	y_1	P/bar
$T = 25.0\text{ }^\circ\text{C}$					
0.0000	0.0000	6.0	0.0667	0.8366	61.9
0.0096	0.5462	15.1	0.0808	0.8472	72.3
0.0196	0.6863	23.4	0.0935	0.8531	82.9
0.0294	0.7483	31.9	0.1038	0.8572	91.4
0.0415	0.7971	41.7	0.1178	0.8619	102.4
0.0550	0.8245	52.6			
$T = 35.0\text{ }^\circ\text{C}$					
0.0000	0.0000	7.8	0.0706	0.7971	65.8
0.0092	0.4716	16.5	0.0824	0.8054	73.1
0.0174	0.5962	23.2	0.0947	0.8155	82.9
0.0255	0.6745	30.7	0.1112	0.8207	95.3
0.0385	0.7352	41.1	0.1243	0.8240	103.5
0.0529	0.7723	52.6			
$T = 45.0\text{ }^\circ\text{C}$					
0.0000	0.0000	10.0	0.0488	0.6997	49.0
0.0052	0.2735	15.0	0.0630	0.7300	58.9
0.0121	0.4488	20.9	0.0812	0.7559	72.8
0.0220	0.5599	28.3	0.0969	0.7667	83.0
0.0308	0.6230	34.9	0.1116	0.7756	92.8
0.0384	0.6599	40.4	0.1265	0.7796	102.1

Table 5. Compositions of the Liquid 1 (x_1 , x_2), Liquid 2 (x_1 , x_2), and Vapor (y_1 , y_2) Phases at the Pressure P for the System N_2 (1) + $(CH_3)_2O$ (2) + H_2O (3)

lower liquid		upper liquid		vapor		P/bar
x_1	x_2	x_1	x_2	y_1	y_2	
$T = 25.0\text{ }^\circ\text{C}$						
0.0000	0.1468	0.0000	0.8580	0.0000	0.9978	5.6
0.0003	0.1704	0.0037	0.8455	0.4744	0.5224	19.2
0.0004	0.1613	0.0108	0.8402	0.6734	0.3249	41.5
0.0006	0.1561	0.0178	0.8491	0.7269	0.2714	60.5
0.0008	0.1503	0.0265	0.8384	0.7548	0.2398	80.7
0.0012	0.1500	0.0363	0.8427	0.7691	0.2289	98.5
$T = 35.0\text{ }^\circ\text{C}$						
0.0000	0.1448	0.0000	0.8318	0.0000	0.9913	7.3
0.0001	0.1477	0.0023	0.8134	0.3219	0.6705	16.8
0.0001	0.1491	0.0044	0.8235	0.4426	0.5514	23.7
0.0003	0.1458	0.0085	0.8166	0.5655	0.4268	36.7
0.0004	0.1403	0.0140	0.8308	0.6318	0.3629	51.3
0.0005	0.1373	0.0194	0.8197	0.6705	0.3266	64.8
0.0008	0.1348	0.0259	0.8141	0.6950	0.3006	81.2
0.0012	0.1426	0.0354	0.8273	0.7083	0.2878	99.6
$T = 45.0\text{ }^\circ\text{C}$						
0.0000	0.1317	0.0000	0.8139	0.0000	0.9921	9.4
0.0001	0.1346	0.0028	0.8213	0.2878	0.7046	20.4
0.0003	0.1309	0.0097	0.8327	0.5046	0.4887	41.0
0.0006	0.1272	0.0174	0.8255	0.5981	0.3992	61.4
0.0008	0.1247	0.0264	0.8183	0.6341	0.3621	80.5
0.0010	0.1180	0.0368	0.8271	0.6479	0.3486	99.3

This method of calibration requires that the density of the compound be known at the conditions where the calibration is performed. The density of DME was taken from ref 7. The densities of water and methanol were taken from ref 8. The density of CO_2 was taken from ref 9, and the density of N_2 was taken from ref 10.

Sampling from the Autoclave. When taking a liquid sample, the height of the sampling needle was adjusted so that the tip of the needle was located in the liquid phase that was to be measured. Liquid was recycled through the liquid sampling valve using the liquid pump. When the liquid sampling valve was turned, the liquid sample entered the He stream and was carried into the GC.

Vapor samples were taken through a hole in the lid and were led to the on-off valve and vapor valve by a $1/16$ in. pipe. Both the pipe and valves were heated to 20 K above the temperature of the autoclave to ensure that no liquid

Table 6. Compositions of the Liquid 1 (x_1 , x_2), Liquid 2 (x_1 , x_2), and Vapor (y_1 , y_2) Phases at the Pressure P for the System CO_2 (1) + $(CH_3)_2O$ (2) + H_2O (3)

lower liquid		upper liquid		vapor		P/bar
x_1	x_2	x_1	x_2	y_1	y_2	
$T = 25.0\text{ }^\circ\text{C}$						
0.0000	0.1793	0.0000	0.7231	0.0000	0.9900	5.4
0.0098	0.1100	0.1538	0.7231	0.5739	0.4230	11.8
0.0129	0.0664	0.3575	0.5991	0.7845	0.2141	20.7
0.0272	0.0462	0.5484	0.4259	0.8661	0.1316	29.5
0.0349	0.0280	0.6916	0.2898	0.9117	0.0856	39.4
0.0428	0.0160	0.7945	0.1661	0.9480	0.0520	48.6
$T = 35.0\text{ }^\circ\text{C}$						
0.0000	0.1142	0.0000	0.8274	0.0000	0.9900	7.5
0.0080	0.0862	0.2172	0.7142	0.6264	0.3644	19.0
0.0164	0.0546	0.4434	0.5227	0.7909	0.1982	31.7
0.0163	0.0288	0.6443	0.3207	0.8727	0.1171	46.0
0.0234	0.0154	0.7867	0.1688	0.9138	0.0732	58.8
$T = 45.0\text{ }^\circ\text{C}$						
0.0000	0.1309	0.0000	0.7683	0.0000	0.9900	9.4
0.0068	0.0886	0.1899	0.7270	0.5622	0.4262	21.4
0.0116	0.0483	0.4189	0.5435	0.7514	0.2425	36.2
0.0155	0.0358	0.5451	0.4303	0.8092	0.1857	45.7
0.0179	0.0133	0.6498	0.3156	0.8528	0.1432	55.9
0.0180	0.0194	0.6828	0.2452	0.8701	0.1243	61.9

Table 7. Compositions of the Liquid (x_1 , x_2 , x_3) and Vapor (y_1 , y_2 , y_3) Phases at the Pressure P for the System N_2 (1) + $(CH_3)_2O$ (2) + H_2O (3) + CH_3OH (4)

liquid			vapor			P/bar
x_1	x_2	x_3	y_1	y_2	y_3	
$T = 25.0\text{ }^\circ\text{C}$						
0.0000	0.2359	0.6358	0.0000	0.9897	0.0031	4.8
0.0004	0.2533	0.6241	0.5787	0.4136	0.0042	22.4
0.0011	0.2600	0.6069	0.7094	0.2816	0.0046	41.5
0.0015	0.2454	0.6262	0.7623	0.2324	0.0034	60.9
0.0020	0.2474	0.6209	0.7837	0.2103	0.0032	80.5
0.0025	0.2463	0.6229	0.7973	0.1982	0.0024	102.1
$T = 35.0\text{ }^\circ\text{C}$						
0.0000	0.3123	0.5308	0.0000	0.9771	0.0101	6.8
0.0005	0.3015	0.5430	0.4197	0.5654	0.0067	17.8
0.0013	0.2972	0.5469	0.6096	0.3810	0.0045	34.2
0.0019	0.3014	0.5430	0.6770	0.3146	0.0041	48.2
0.0026	0.3062	0.5373	0.7126	0.2788	0.0041	60.7
0.0037	0.3199	0.5195	0.7444	0.2497	0.0024	82.3
0.0044	0.3036	0.5444	0.7562	0.2354	0.0043	98.6
$T = 45.0\text{ }^\circ\text{C}$						
0.0000	0.2630	0.6392	0.0000	0.9795	0.0098	8.2
0.0006	0.2896	0.5888	0.4432	0.5399	0.0106	27.2
0.0012	0.2696	0.6290	0.5658	0.4232	0.0063	42.5
0.0017	0.2739	0.6221	0.6354	0.3544	0.0053	61.7
0.0025	0.2758	0.6177	0.6792	0.3105	0.0057	81.2
0.0031	0.2650	0.6246	0.6889	0.3007	0.0057	99.5

dropout occurred when taking samples from the cell. The loop was filled with sample by letting vapor from the cell flow through it and into a beaker filled with water until the pipe and valve were flushed. When the vapor valve was turned, the vapor sample entered the He stream and was carried into the GC. For all points, two samples were taken and an average was used as the result. The deviation between the points was normally within 1 to 2% while points measured at the detection limit of the GC would show a deviation up to 50%.

Uncertainty. The uncertainty of the measured mole fractions is estimated to be 3%, while the reproducibility was found to be within 1.5%. The uncertainty was found to depend on which phase was measured. The vapor had the smallest uncertainty, averaging 1% for the light component and 25% for the heavy components. The large number for the heavy components was due to the small amount present in the vapor phase, leading to measure-

Table 8. Compositions of the Liquid 1 (x_1, x_2, x_3), Liquid 2 (x_1, x_2, x_3), and Vapor (y_1, y_2, y_3) Phases at the Pressure P for the System CO_2 (1) + $(\text{CH}_3)_2\text{O}$ (2) + H_2O (3) + CH_3OH (4)^a

lower liquid			upper liquid			vapor			P/bar
x_1	x_2	x_3	x_1	x_2	x_3	y_1	y_2	y_3	
$T = 25.0\text{ }^\circ\text{C}$									
0.0000	0.1467	0.7449	***	***	***	0.0000	0.9861	0.0061	4.6
0.0174	0.1220	0.7469	0.2339	0.5383	0.1611	0.7412	0.2469	0.0089	18.3
0.0213	0.0704	0.7748	0.4442	0.4515	0.0549	0.8507	0.1435	0.0029	27.7
0.0306	0.0313	0.8163	0.6442	0.2615	0.0611	0.9154	0.0759	0.0049	40.1
0.0434	0.0225	0.8095	0.6731	0.1844	0.1123	0.9339	0.0556	0.0074	45.2
$T = 35.0\text{ }^\circ\text{C}$									
0.0000	0.1100	0.4145	***	***	***	0.0000	0.9797	0.0071	5.8
0.0356	0.1475	0.6607	0.2288	0.4636	0.2014	0.7451	0.2449	0.0044	24.6
0.0311	0.0802	0.7366	0.4210	0.4272	0.0740	0.8281	0.1623	0.0050	34.2
0.0282	0.0523	0.7590	0.5538	0.3363	0.0493	0.8712	0.1187	0.0048	42.5
0.0350	0.0337	0.7644	0.6883	0.2435	0.0258	0.9040	0.0856	0.0055	51.3
$T = 45.0\text{ }^\circ\text{C}$									
0.0000	0.2073	0.6840	***	***	***	0.0000	0.9789	0.0093	8.0
0.0229	0.1745	0.6856	0.1293	0.5047	0.2767	0.6080	0.3814	0.0048	21.6
0.0281	0.0930	0.7707	0.3220	0.4515	0.1607	0.7609	0.2244	0.0091	34.9
0.0259	0.0493	0.8039	0.5292	0.3484	0.0764	0.8354	0.1533	0.0053	48.1
0.0287	0.0380	0.8087	0.6312	0.2984	0.0323	0.8607	0.1275	0.0058	55.6

^a *** means phase not present.

Table 9. Compositions of the Liquid 1 (x_1, x_2, x_3, x_4), Liquid 2 (x_1, x_2, x_3, x_4), and Vapor (y_1, y_2, y_3, y_4) Phases at the Pressure P for the System N_2 (1) + CO_2 (2) + $(\text{CH}_3)_2\text{O}$ (3) + H_2O (4) + CH_3OH (5)^a

lower liquid				upper liquid				vapor				P/bar
x_1	x_2	x_3	x_4	x_1	x_2	x_3	x_4	y_1	y_2	y_3	y_4	
$T = 25.0\text{ }^\circ\text{C}$												
0.0000	0.0000	0.1697	0.6769	***	***	***	***	0.0000	0.0000	0.9845	0.0044	4.4
0.0000	0.0289	0.1266	0.6869	0.0000	0.2829	0.4873	0.1345	0.0000	0.7983	0.1966	0.0024	21.6
0.0003	0.0261	0.1136	0.7071	0.0064	0.2495	0.4692	0.1774	0.2529	0.5768	0.1663	0.0014	42.6
0.0005	0.0250	0.1241	0.6865	0.0118	0.2614	0.5107	0.1189	0.3352	0.5039	0.1562	0.0016	56.9
0.0008	0.0250	0.1250	0.6853	0.0170	0.2571	0.5126	0.1184	0.4439	0.3962	0.1544	0.0022	70.5
0.0011	0.0256	0.1300	0.6936	0.0227	0.2514	0.5168	0.1162	0.4866	0.3520	0.1551	0.0017	84.3
0.0013	0.0229	0.1298	0.6887	0.0291	0.2448	0.5230	0.1111	0.5226	0.3154	0.1561	0.0024	99.4
$T = 35.0\text{ }^\circ\text{C}$												
0.0000	0.0000	0.1747	0.6660	***	***	***	***	0.0000	0.0000	0.9762	0.0088	5.6
0.0000	0.0343	0.1241	0.6773	0.0000	0.2963	0.4678	0.1335	0.0000	0.7837	0.2073	0.0036	27.9
0.0003	0.0310	0.1187	0.6927	0.0055	0.2676	0.4515	0.1728	0.1781	0.6247	0.1868	0.0041	45.8
0.0009	0.0343	0.1321	0.6663	0.0137	0.2665	0.4616	0.1567	0.2920	0.5271	0.1708	0.0052	67.7
0.0012	0.0296	0.1267	0.6732	0.0189	0.2509	0.4653	0.1634	0.3926	0.4139	0.1815	0.0067	81.8
0.0014	0.0254	0.1358	0.6708	***	***	***	***	0.4383	0.3672	0.1842	0.0046	92.5
$T = 45.0\text{ }^\circ\text{C}$												
0.0000	0.0000	0.1620	0.7028	***	***	***	***	0.0000	0.0000	0.9734	0.0115	7.3
0.0000	0.0362	0.1398	0.6951	0.0000	0.2480	0.4889	0.1634	0.0000	0.7290	0.2589	0.0061	30.3
0.0003	0.0288	0.1272	0.7073	0.0061	0.2321	0.4983	0.1622	0.1725	0.5797	0.2363	0.0057	49.3
0.0008	0.0257	0.1306	0.6952	0.0108	0.2070	0.4823	0.1977	0.2582	0.4955	0.2320	0.0083	64.5
0.0009	0.0248	0.1308	0.6875	***	***	***	***	0.3160	0.4462	0.2246	0.0073	76.5
0.0012	0.0200	0.1277	0.6937	***	***	***	***	0.3722	0.3997	0.2152	0.0058	94.8

^a *** means phase not present.

ments close to the limit of the used GC detector. The liquid phases were found to have an average uncertainty of 3%. The uncertainty of the temperature was found to be 0.2 K, while the uncertainty of the pressure measurements was found to be 0.1 bar.

Procedures. The system was evacuated for several hours before use to remove any traces of gas. Liquid samples were added to the cell using the vacuum to draw the liquid into the cell. When there was to be water in the cell, sufficient water was added so that its level would reach above the lower window edge to ensure that any phase split could be seen. The gases were added from high-pressure supply bottles. When CO_2 was needed at pressures above about 55 bar, an ISCO pump model 260D syringe pump was used to supply the desired pressure. After the compounds were added, the autoclave was thermostated overnight and samples were taken from each phase as described above. The next point was reached by adding either CO_2

or N_2 to the system until the desired pressure level was reached. After the pressure was reached, the cell contents were mixed for 10 min and left for a minimum of 2 h to reach equilibrium. Depending on the separation time needed on the GC, either one or two points could be measured each day. The calibration did not take any additional time, since it was done while the system was awaiting equilibrium.

Materials. The materials used are listed in Table 1. The purity of the materials was checked using the GC, and they were used without any further purification.

Results and Discussion

To test the equipment and procedure, two well-known systems were measured at first. Figure 3 shows a comparison between measured data and four sets of literature data for the system $\text{CO}_2 + \text{CH}_3\text{OH}$ at 25.0 °C. The

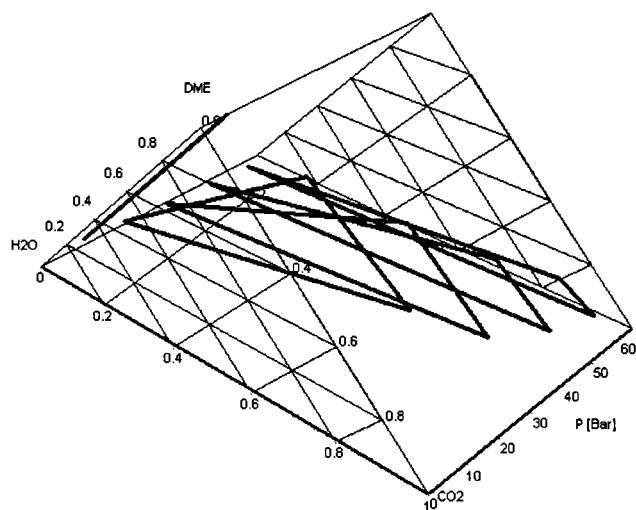


Figure 5. 3D chart showing the VLLE system CO_2 (1) + $(\text{CH}_3)_2\text{O}$ (2) + H_2O (3) at 35.0 °C

measured data are given in Table 2. Good agreement was obtained, but because of the large scatter of the data available for this system, the system CO_2 + $(\text{CH}_3)_2\text{O}$ was also measured in order to verify the equipment and method. Figure 4 shows a comparison between literature data and data obtained in this work for the system CO_2 + $(\text{CH}_3)_2\text{O}$ at 47.0 °C. As can be seen, good agreement was achieved. The measured data are given in Table 3.

Following the verification, the system N_2 + $(\text{CH}_3)_2\text{O}$ was measured. This system shows only VLE behavior. The measured data are given in Table 4.

The system N_2 + $(\text{CH}_3)_2\text{O}$ + H_2O shows VLLE behavior; see Table 5. N_2 has little effect on the composition of the two liquid phases while the vapor phase becomes enriched in N_2 .

The system CO_2 + $(\text{CH}_3)_2\text{O}$ + H_2O shows VLLE behavior due to the poor miscibility between water and DME; see Figure 5 and Table 6. When these measurements were performed, the water rich phase showed little change when increasing the pressure by adding CO_2 to the cell, while the DME rich phase expanded, until the system was at the limit of becoming an LLE system.

The system N_2 + $(\text{CH}_3)_2\text{O}$ + H_2O + CH_3OH showed only VLE behavior. This was believed to be due to the amount of methanol in the system; see Table 7. As the numbers show, the only major change when increasing the pressure is the lowering of the DME mole fraction in the vapor phase. The liquid phase showed only minor changes.

The system CO_2 + $(\text{CH}_3)_2\text{O}$ + H_2O + CH_3OH showed both VLE and VLLE behavior; see Table 8. Before CO_2 was added to the cell, a VLE system was found because of the presence of methanol. When CO_2 was added, a second liquid phase split out. As the pressure was increased by adding CO_2 to the cell, the DME content of the water rich liquid phase was found to decrease. The vapor phase became richer in CO_2 ; the same was found in the DME rich liquid phase. As the pressure was increased, the DME rich liquid phase expanded until the system was on the limit of becoming an LLE system and the measurement was stopped.

The system N_2 + CO_2 + $(\text{CH}_3)_2\text{O}$ + H_2O + CH_3OH was measured by adding water, methanol, and DME to the cell. CO_2 was then added until a second liquid phase split out. Thereafter, the pressure was increased by adding N_2 ; see Table 9. It was seen in the cell that the DME rich phase became smaller when the pressure was increased, and in

some cases the system reverted to a VLE system at elevated pressures.

Conclusions

Equipment for measuring both VLE and VLLE phase equilibria has been developed. It has been demonstrated that the use of on-line sampling combined with pure-component calibration can provide both fast and reliable experimental data. The method has been validated by measuring the system CO_2 + $(\text{CH}_3)_2\text{O}$ at 47.0 °C and the system CO_2 + CH_3OH at 25.0, 30.0, and 40.0 °C. The measured data show good agreement with literature data. Isotherms at 25.0, 35.0, and 45.0 °C are presented for the systems N_2 + $(\text{CH}_3)_2\text{O}$, N_2 + $(\text{CH}_3)_2\text{O}$ + H_2O , CO_2 + $(\text{CH}_3)_2\text{O}$ + H_2O , CO_2 + $(\text{CH}_3)_2\text{O}$ + H_2O + CH_3OH , N_2 + $(\text{CH}_3)_2\text{O}$ + H_2O + CH_3OH , and N_2 + CO_2 + $(\text{CH}_3)_2\text{O}$ + H_2O + CH_3OH ; of these only data for N_2 + $(\text{CH}_3)_2\text{O}$ have previously been published.

Literature Cited

- (1) Hansen, J. B.; Voss, B.; Joensen, F.; Sigurdardottir, I. Large Scale Manufacture of Dimethyl Ether. A new alternative diesel fuel from natural gas. SAE Paper No. 950063, 1995.
- (2) Jonasson, A.; Persson, O.; Fredenslund, Aa. High-Pressure Solubility of Carbon Dioxide and Carbon Monoxide in Dimethyl Ether. *J. Chem. Eng. Data* **1995**, *40*, 296–300.
- (3) Jonasson, A.; Persson, O.; Rasmussen, P. High-Pressure Solubility of Hydrogen in Dimethyl Ether. *J. Chem. Eng. Data* **1995**, *40*, 1209–1210.
- (4) Teodorescu, M.; Rasmussen, P. High-Pressure Vapour-Liquid Equilibria in the Systems Nitrogen + Dimethyl Ether, Methanol + Dimethyl Ether, Carbon Dioxide + Dimethyl Ether + Methanol, and Nitrogen + Dimethyl Ether + Methanol. *J. Chem. Eng. Data* **2001**, *46* (3), 640–646.
- (5) Holldorff, H.; Knapp, H. Binary Vapour-Liquid-Liquid Equilibrium of Dimethyl Ether-Water and Mutual Solubilities of Methyl Chloride and Water. *Fluid Phase Equilib.* **1988**, *44*, 195–209.
- (6) Elbaccouch, M. M.; Elliott, J. R. High-Pressure Vapour-Liquid Equilibrium for Dimethyl Ether + Ethanol and Dimethyl Ether + Ethanol + Water. *J. Chem. Eng. Data* **2000**, *45*, 1080–1087.
- (7) Haworth, W. S.; Sutton, L. E. Equilibrium of Polar Gases. *Trans. Faraday Soc.* **1971**, *586* (67), 2901–2914.
- (8) Design Institute for Physical Property Data (DIPPR), AIChE, 1989.
- (9) Angus, S. B.; Armstrong, B.; de Reuck, K. M. Carbon dioxide. *International Thermodynamic Tables of the Fluid State-3*, IUPAC; Pergamon Press: Oxford, 1976.
- (10) Angus, S. B.; Armstrong, B.; de Reuck, K. M. Nitrogen. *International Thermodynamic Tables of the Fluid State-6*, IUPAC; Pergamon Press: Oxford, 1979.
- (11) Chang, C. J.; Day, C.; Ko, C.; Chiu, K. Densities and P-x-y Diagrams for Carbon Dioxide Dissolution in Methanol, Ethanol, and Acetone Mixtures. *Fluid Phase Equilib.* **1997**, *131*, 243–258.
- (12) Ohgaki, K.; Katayama, T. Isothermal Vapour-Liquid Equilibria Data for Binary Systems Containing Carbon Dioxide at High Pressures: Methanol-Carbon Dioxide, n-Hexane-Carbon Dioxide, and Benzene-Carbon Dioxide Systems. *J. Chem. Eng. Data* **1976**, *21* (1), 53–55.
- (13) Katayama, T.; Ohgaki, K.; Maekawa, G.; Goto, M.; Nagano, T. Isothermal Vapour-Liquid Equilibria of Acetone-Carbon Dioxide and Methanol-Carbon Dioxide Systems at High Pressures. *J. Chem. Eng. Jpn.* **1975**, *8*, 89–92.
- (14) Brunner, E.; Hultenschmidt, W.; Schlichthärle, G. Fluid Mixtures at High Pressures IV. Isothermal Phase Equilibria in Binary Mixtures Consisting of (Methanol + Hydrogen or Nitrogen or Methane or Carbon Monoxide or Carbon Dioxide). *J. Chem. Thermodyn.* **1987**, *19*, 273–291.
- (15) Tsang, C. Y.; Streett, W. B. Vapour-Liquid Equilibrium in the System Carbon Dioxide/Dimethyl Ether. *J. Chem. Eng. Data* **1981**, *26*, 155–159.

Received for review May 16, 2001. Accepted November 14, 2001. The authors wish to thank Haldor Topsøe A/S for financial support of the project.

JE010154-